Original Article

Institution of MECHANICAL ENGINEERS
Journal of AEROSPACE ENGINEERING

Proc IMechE Part G:
J Aerospace Engineering
2019, Vol. 233(3) 896–907

DOI: 10.1177/0954410017742932
journals.sagepub.com/home/pig
SAGE

Mass properties identification and automatic mass balancing system for satellite attitude dynamics simulator

Ghasem Sharifi, Mehran Mirshams and Hamed Shahmohamadi Ousaloo

Abstract

A Satellite Attitude Dynamics Simulator is a low-cost, ground-based system made to simulate the conditions of a weightless satellite in space. The identification of the mass characteristics is crucial for Satellite Attitude Dynamics Simulator application and so the center of mass place is necessary for balancing the platform and moment of inertia which is a significant factor in designing controllers and selecting actuators. The purposes of this paper are the mass properties identification and design, experimentation, and validation of an automatic mass balancing system, which is assembled on the Satellite Attitude Dynamics Simulator at the Space Research Laboratory. This paper presents a process of mass properties estimation for the Satellite Attitude Dynamics Simulator using classical Levenberg–Marquardt as an optimization method. By employing this technique lack of repeatability and difficulties in implementation will be eliminated. In order to verify this technique, a MATLAB® SIMULINK® model of the Satellite Attitude Dynamics Simulator is established. The gap between the center of mass and center of rotation is decreased by means of the automatic mass balancing system in order to remove gravity disturbance. The results of this identification process are compared to the recursive least square algorithm, which is commonly employed in identification of mass properties. The analytical and experimental results prove that the proposed characteristic estimation process using classical Levenberg–Marquardt algorithm is more effective and appropriate. Proper excitation of the platform will guarantee the accuracy of estimation and compensation of the center of gravity offset utilizing the balancing system.

Keywords

Satellite Attitude Dynamics Simulator, parameter estimation, automatic mass balancing system, attitude control, Levenberg–Marquardt algorithm, air bearing

Date received: 28 May 2017; accepted: 20 October 2017

Introduction

Owing to great difficulties in changing satellite structure and reconfiguration in space, ground simulations and testing are highly necessary. In the past three decades, Satellite Attitude Dynamic Simulator (SADS) has been commonly used to test and validate the system's performance under a circumstance similar to its real work conditions to eliminate the errors of control algorithms and devices.[1–6] Using the air bearing is an essential part of the process for developing and testing attitude control system algorithms. The SADS commonly uses air bearing to suspend the platform and simulate frictionless and micro-gravity space environments. Air bearing uses a thin film of pressurized air to provide an exceedingly low friction interface between surfaces. In this device, a compressor provides compressed air that passes through pores on the bearing surface and creates a thin film of air which endures the weight of movable parts and sustains the platform without any shear stress on the bearing. The frictionless nature of the air bearing nearly simulates a zero-g environment, allowing the pitch, roll, and yaw control systems of the satellite to function as they would in space. These bearings are classified into two types: planar and spherical. The planar air bearings are common systems to provide three degrees of freedom as one rotational and two translational, which are employed for experimental testing of formation flying, rendezvous, and docking. Because of the ability to provide 3DOF rotational

Department of the Aerospace Engineering, K.N. Toosi University of Technology, Tehran, Iran

Corresponding author:
Ghasem Sharifi, K. N. Toosi University of Technology, Tehran 19697, Iran.
Email: ghsm.sharifi@gmail.com

motion, spherical air bearing systems are used for satellite attitude control simulations.[7] There are varieties of disturbance elements which reduce the performance of the SADS. Disturbances of the SADS are divided into four categories: structure, air bearing, environmental, and test condition,[8] while the most significant disturbance is caused by the unbalanced mass of the structure. The gap between the center of rotation (CR) and center of mass (CM) creates the unbalancing.

In order to balance the SADS, both manual and automatic approaches are used. Although the manual balancing is a low-cost approach and does not demand advanced technology and skills, it is a time-consuming process and usually does not have appropriate accuracy. High accuracy in the mass balancing in a short time interval can be achieved by means of an automatic balancing method. In this method, three balance masses along three axes are moved by the stepper motors to reduce the gravity torque. Direct estimation of the mass center is frequently applied in the automatic mass balancing.

In order to compensate for the unbalanced disturbances, the required displacements of the balance masses must be determined. Modeling the SADS in the computer-aided design (CAD) software is one of the approaches to determine the mass properties.[9,10] Despite the advantages of the CAD software such as financial cost, there are some errors caused by inaccuracy in the modeling of the equipment. To overcome the difficulties associated with the manual balancing, many authors have considered automatic mass balancing systems (AMBSs) as a beneficial solution.

In Small and Zajac[11] a linear controller was designed and the balance masses acted as actuators to remove the disturbance torques. In this technique, first the platform was located in horizontal position and the gravitational torques were calculated. After that, two masses along the two axes were moved to the desired location to balance the structure. This procedure is repeated to meet the exact balancing. Employing this time-consuming technique, the mass properties cannot be obtained.

An adaptive control method is presented in Kim and Agrawal.[7] The approach is based on moving the balance masses in a desired path, in which the total angular momentum of the system remains constant. In this method, satellite simulator is excited continuously with a preplanned satellite momentum trajectory and no external torques are applied on the simulator. By determining the difference between the measured and preplanned momentum trajectories, the balance masses are actuated in order to remove this residual. Its challenge is processing high volume of data and difficulty in the strategy implementation.

In Ma et al.[12] one momentum technique has been applied to estimate spacecraft inertia using a robotic arm to change the velocity of the spacecraft. Least squares estimation (LSE) technique is the main method for the mass properties identification. By using the LSE method, the center of gravity and the moment of inertia are directly estimated and the new position of the balance masses is determined to remove the distance between the CM and CR.[10,13–16] In De Oliveira et al.[17,18] the mass properties are estimated by the extended Kalman filter and recursive least squares (RLS). In this study, the refinement of the extended Kalman filter was more than the LSE method in the experimental result on the planar and dumbbell shape of the SADS. The RLS parameter estimation algorithm has been employed to identify the mass properties in Jung and Tsiotras[19] and it has been shown that the mass properties at each sample time can be estimated. The identification issue was converted into a nonlinear optimal problem and particle swarm optimization algorithm was used to estimate the CM and inertia parameters.[20]

Although LSE method has been employed for identification processes in other SADS, this method has some disadvantages that precise results cannot be obtained conveniently and numerous experiments should be applied on the SADS to find reliable data. Furthermore, sometimes provided results are not acceptable. This problem has been reported in the SADS for Virginia Tech and INPE Institute[10,17] and for our study in this paper as well. Because of this major problem of the LSE approach, we propose the new process and technique for the identifiying and balancing the SADS with accurate results. The advantage of this approach is that by an adequate excitation of the SADS about three axes, the results of estimation will be accurate and reliable. Moreover, the implementation of the optimization technique is more convenient and this method has a suitable speed run. This method is less sensible on the external effect and is useful for a system with unknown disturbance. Also, in most research studies, authors have just used techniques to determine mass properties and have not considered balance mechanism and procedure of balancing system. The processes of mass balancing are clearly explained in this research.

The objective of this work is to validate the AMBS of the Space Research Laboratory (SRL) SADS. A balance mechanism in order to remove the gravity disturbance by moving of three balance masses is designed and assembled on the platform. The SADS is excited by three orthogonal reaction wheels, while the angular velocity and Euler angles are measured by an Attitude and Heading Reference System (AHRS). The classical Levenberg–Marquardt (CLM) and RLS methods are implemented to identify the mass properties of the SRL SADS including the position of the CM and the moment of inertia tensor; in line with this, the estimated results of two methods are compared. The CM of the SADS is then moved near the CR by employment of AMBS which is adjusted to the precise location and this procedure is iterated until the gravitational torque level converges to its minimum value.

The SADS model

SRL has developed a 3DOF dumbbell-shaped satellite simulator with the aim of evaluation for development of satellite attitude control system, various controllers, and novel algorithms for switching between actuators in an experimental system.[21] Furthermore, the SADS is used to present the principles of attitude dynamics, satellite operational environment, application of actuators and sensors and development of control methods by students and experts at SRL. Hardware located on the SADS includes thrusters, two nitrogen tanks, a microcontroller, lead–acid batteries, power control unit, three reaction wheels, remote communication devices, AMBS and AHRS for attitude determination (see Figure 1). Attitude control options include three reaction wheels and 16 cold gas thrusters. In this research, reaction wheels are used for estimation of the mass parameters which will excite the SADS.

Equation of motion for the platform

The SADS is a rigid body in which control and disturbance torques are applied to the platform. The significant environmental torque affecting the platform is due to gravity. The origin of the reference body frame {B} is located at the pivot. The Euler's equation describes the dynamic of the satellite simulator as follows[22]

$$M = \left(\frac{\mathrm{d}\vec{H}}{dt}\right)_I = \left(\frac{\mathrm{d}\vec{H}}{dt}\right)_b + \left(\omega \times \vec{H}\right) \tag{1}$$

where M is the external torque applied to the system, $\vec{H}$ is the total angular momentum, and ω is the angular rate of the simulator in its body reference system.

Total angular momentum of the satellite simulator includes the angular momentum of the platform and angular momentum of the reaction wheels as described by equation (2)

$$\vec{H} = \vec{h}_I + \vec{h}_{rw} \tag{2}$$

where $\vec{h}_I$ is the angular momentum of the platform and $\vec{h}_{rw}$ is the angular momentum of the reaction wheel. The offset between CM and CR produces a gravitational torque acting as an disturbance torque and is represented by equation (3)

$$M = \vec{r} \times m\vec{g} \tag{3}$$

where $\vec{r}$ is a vector from CM to CR in the body coordinate system, m is the total mass of the system, and $\vec{g}$ is the local gravitational acceleration vector. Inserting equations (2) and (3) in equation (1), the dynamics of the satellite simulator under the gravity torque is represented by equation (4) as follows

$$\vec{r} \times m\vec{g} = J\dot{\vec{\omega}} + \vec{\omega} \times J\vec{\omega} + \dot{\vec{h}}_{rw} + \vec{\omega} \times \vec{h}_{rw} \tag{4}$$

Parameter estimation techniques

RLS technique

The RLS technique is one of the best known and common algorithms used in adaptive filtering and system identification.[23] The importance of this

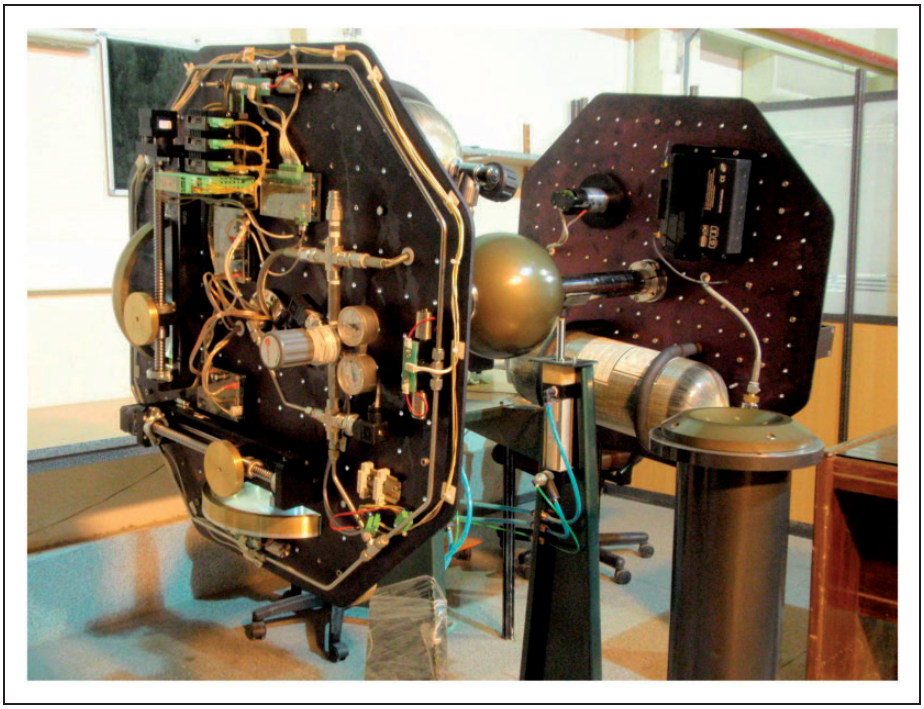

Figure 1. The SRL satellite attitude and dynamics simulator.

algorithm is due to their low complexity and easy implementation characteristics. In this method, the estimated parameters are computed recursively in each sample time: suppose that there exist an estimated x_{t-1} at iteration -1, then recursive identification aims to compute a new estimated x_t by a "simple modification" of x_{t-1} when a new measured data become available at iteration t. Equation (5) can be rewritten as[15]

$$\dot{\Omega}J + \omega \times \Omega J + [g\times]mr = -\dot{h}_{r\omega} - \omega \times h_{r\omega} \tag{5}$$

where J, $[g\times]$, and Ω are defined as follows

$$\Omega = \begin{bmatrix} \omega_1 & 0 & 0 & \omega_2 & \omega_3 & 0 \\ 0 & \omega_2 & 0 & \omega_1 & 0 & \omega_3 \\ 0 & 0 & \omega_3 & 0 & \omega_1 & \omega_2 \end{bmatrix}$$

$$J = \begin{bmatrix} J_{xx} & J_{yy} & J_{zz} & J_{xy} & J_{xz} & J_{yz} \end{bmatrix}^T$$

$$[g\times] = \begin{bmatrix} 0 & -g_3 & g_2 \\ g_3 & 0 & -g_1 \\ -g_2 & g_1 & 0 \end{bmatrix} \tag{6}$$

Gravity torque is applied to the rigid body, hence we need to transform gravitational acceleration vector from local inertial frame to the body reference system

$$[g\times] = g\begin{bmatrix} 0 & -c(\emptyset)c(\theta) & s(\emptyset)c(\theta) \\ c(\emptyset)c(\theta) & 0 & s(\theta) \\ -s(\emptyset)c(\theta) & -s(\theta) & 0 \end{bmatrix} \tag{7}$$

where s and c represent sin and cos of angle, respectively. Equation (5) can be rewritten in regression form

$$\begin{bmatrix} \dot{\Omega} + \omega \times \Omega & [g\times] \end{bmatrix}\begin{bmatrix} J \\ mr \end{bmatrix} = -\dot{h}_{r\omega} - \omega \times h_{r\omega} \tag{8}$$

Since the AHRS measures angular velocity, to avoid numerical derivative of the angular velocity, the simple integration can be considered as[15]

$$\begin{bmatrix} \Omega + \int_{t_0}^{t}([\omega\times]\Omega)dt & \int_{t_0}^{t}[g\times]dt \end{bmatrix}\begin{bmatrix} J \\ mr \end{bmatrix} = -h_{r\omega} - \int_{t_0}^{t}(\omega \times h_{r\omega})dt \tag{9}$$

Equation (9) is in the linear regression form such that A $x = \mathrm{B}$, where the unknown matrix is as $x = \begin{bmatrix} J \\ mr \end{bmatrix}$. The RLS approach starts from a slightly modified loss function

$$V(t) = \sum_{s=1}^{t} \lambda^{t-s}(B_t - {A_t}^T x) \tag{10}$$

The RLS algorithm can be given by[24]

$$\begin{aligned} K(t) &= \frac{\lambda^{-1}P(t-1)A(t)}{1 + \lambda^{-1}A^T(t)P(t-1)A(t)} \\ \propto(t) &= B(t) - A(t)^T x(t-1) \\ x(t) &= x(t-1) + K(t) \propto(t) \\ P(t) &= \lambda^{-1}P(t-1) - \lambda^{-1}K(t)A(t)^T P(t-1) \end{aligned} \tag{11}$$

where $\propto(t)$ is an estimation residual error at the moment t and λ is forgetting factor. If the value of λ is regarded as about 1 ($\lambda = 0.99$ or $\lambda = 0.95$) then the past observations are not considered in the estimation process by increasing time. The advantage of the RLS algorithm is that the inverse of matrices is not required.

CLM technique

The CLM algorithm is a technique which determines the minimum of a multivariate function where the cost function is explained as the sum of squares error of the real and expected data.[25] The CLM interpolates between two optimization algorithms as the Gauss–Newton algorithm (GNA) and the method of gradient descent (GD). The CLM is more robust and effective than the GNA since in many trails it finds a solution even if the initial condition was too far from the final minimum.

The Levenberg–Marquardt method acts more like a GD method when the parameters are far from their optimal value and acts more like the Gauss–Newton method when the parameters are close to their optimal value.

The cost function of this optimization method is defined as

$$\begin{aligned} f(P) &= \sum_{i=1}^{m}\left[\frac{y(t_i) - \tilde{y}(t_i; P)}{\sigma_{yi}}\right]^2 \\ &= y^T W y - 2y^T W\tilde{y} + \tilde{y}W\tilde{y}^T \end{aligned} \tag{12}$$

where σ_{yi} is the error of measurement $y(t_i)$. Typically the weighting matrix W is diagonal with $W = \frac{1}{\sigma_{yi}}$. If the function $\tilde{y}$ is nonlinear with the variable P, then in order to minimize x^2, the iterative procedure by considering the parameters must be performed. The objective of each iteration is to find a perturbation h to the variable P in order to reduce $f(P)$

$$P_{i+1} = P_i + h_{lm} \tag{13}$$

The CLM proposed an algorithm based on this error, whose parameters are updated based on a rule, which is a combination of the mentioned algorithms and is given as

$$\left[J^T W J + \lambda I\right]h_{lm} = J^T W(y - \tilde{y}) \tag{14}$$

where if the algorithmic parameter λ is small then results are updated based on Gauss–Newton and for large values of λ the GD is employed to the updated results. At the beginning of the procedure, a large parameter λ is considered so that for the first updates GD direction is employed.

As the solution improves and the error of real and functional data is decreased, Levenberg–Marquardt method accelerates the solution to the local minimum by means of the GNA.[26,27]

In Marquardt's update equation

$$\left[J^T WJ + \lambda diag\left(J^T WJ\right)\right]h_{lm} = J^T W(y - \tilde{y}) \tag{15}$$

The values of λ are normalized to the values of $J^T WJ$.

According to equation (1), the parameters that should be estimated during CLM method are as follows

$$J = \begin{bmatrix} J_{xx} & J_{yy} & J_{zz} & J_{xy} & J_{xz} & J_{yz} \end{bmatrix}^T$$
$$r = \begin{bmatrix} r_x \\ r_y \\ r_z \end{bmatrix} \tag{16}$$

CM adjustment

To achieve a virtually torque-free environment it is necessary to balance the SADS accurately. The SADS uses three AMBSs in order to reduce the interference of gravitational torque. Impeccable balancing is achieved when the CM coincides with the CR of the platform. For this reason, the SADS includes three sliding AMBSs for accurate balancing. After identification of the gap between CM and CR by the proposed method, it is necessary to find the distance at which the AMBS needs to balance the simulator. The AMBS includes DC stepper motors mounted so that as the motor rotates, the balance mass is moved along the threaded rod. Balance mechanism consists of a microcontroller, stepper motor, ball screw, and balance mass (see Figure 2). The desired position of the AMBS, which is obtained by estimation process, can be commanded to the stepper motor through the microcontroller. Consequently, ball screw converts rotational motion into linear motion and balance mass moves along the shaft. The microcontroller can also control the speed of linear motion. The balance mass of the AMBS is 1.5 kg, the step angle of the stepper motor is 1.8° while the pitch of the mechanism is 0.001 mm.

The length of a mechanism along the X, Y, and Z axes is 20, 30, and 30 cm, respectively. The motion of the stepper motor causes a change at the CM of the SADS. There are three AMBSs on the SADS each which are placed on a different axis. These mechanisms are shown in Figures 3 and 4.

Model estimation and verification

Before the implementation and validation of the AMBS on the platform, an accurate estimation of parameter simulation process is necessary. The parameter identification methods are verified with a SADS MATLAB®/SIMULINK® model. In this section, the SADS model is simulated and parameter estimation is converted to an optimization problem to match the experimental results obtained from the platform. The results from these tests are used to determine the new location of the balance mass in the AMBS. In these experiments, the SADS rotates

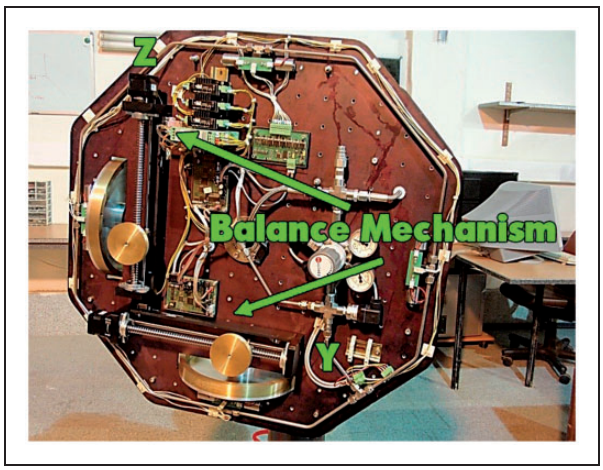

Figure 3. Balance mechanisms along the direction Y and Z.

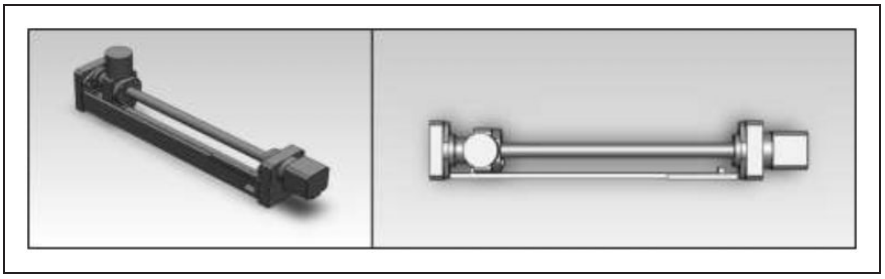

Figure 2. Isometric and top drawing of the balance mechanism in CAD software.

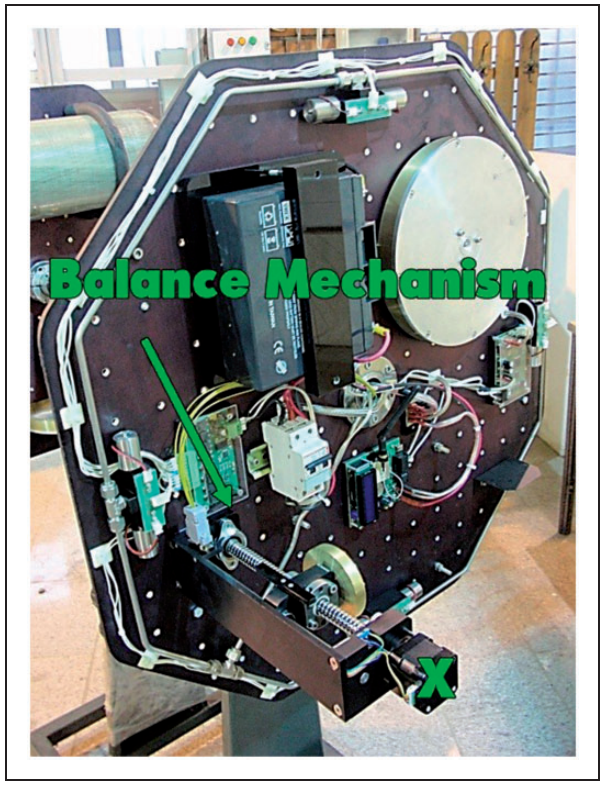

Figure 4. Balance mechanism along the direction X.

Table 1. Results of simulation by RLS and CLM.

Title	Moment of inertia (kg m^2)	Center of mass (m)
RLS	$\begin{bmatrix} 2.97 & -0.1 & 0.05 \\ -0.1 & 11.68 & 0.18 \\ 0.05 & 0.18 & 11.88 \end{bmatrix}$	$\begin{bmatrix} 9.65e-05 \\ -9.36e-05 \\ -0.00032 \end{bmatrix}$
CLM	$\begin{bmatrix} 3.017 & -0.07 & 0.1 \\ -0.07 & 11.79 & 0.18 \\ 0.1 & 0.18 & 11.93 \end{bmatrix}$	$\begin{bmatrix} 9.73e-05 \\ -9.61e-05 \\ -0.00029 \end{bmatrix}$
True	$\begin{bmatrix} 3 & 0 & 0 \\ 0 & 12 & 0 \\ 0 & 0 & 12 \end{bmatrix}$	$\begin{bmatrix} 0.0001 \\ -0.0001 \\ -0.0003 \end{bmatrix}$

CLM: classical Levenberg–Marquardt; RLS: recursive least squares.

by three reaction wheels with maximum momentum capacity of 5 N ms commanded by a simple quaternion-based proportional-derivate (PD) controller to track defined targets and during this maneuver the mass center and moment of inertia are estimated. The true values of the simulated SADS parameters used in the simulation are summarized in Table 1.

In order to predict the realistic performance and efficiency of the techniques, the noise of the AHRS should be considered. The noise level of the Euler angles and angular rate are, respectively, 2° and 0.25°/s. Moreover, the uncertain disturbance torques acting on the SADS are considered between −0.01 and 0.01 N m. Simulation executed in SIMULINK and fourth-order Runge–Kutta method is employed as a solver, furthermore the step size is considered as 0.2 s. The results of the simulations are presented in Table 1.

As can be seen in Table 1, the results of the simulation confirm that both methods could identify mass properties with acceptable accuracy. Both two estimation schemes are capable of producing highly accurate estimations of the moments and products of inertia as well as the mass center of the simulated SADS. The CLM converged to the true inertia parameters closer than any other method.

After simulation, the satisfactory identification results are demonstrated by the model validation in Figure 5. The angular velocities of the simulated SADS using the presented techniques are shown in Figure 5.

Two methods are tracking the real angular velocity with sufficient accuracy. The accuracy of the estimation is a function of the noises and disturbances.

Experimental application

Mass properties identification

Accurate determination of the SADS's mass property using CAD® model is not possible, owing to the diversity of the installed equipment and inaccurate modeling of the devices. In order to estimate the moment of inertia tensor and the location of mass center, the already mentioned estimation methods are used. Since the geometric shape of the reaction wheel is simple (Figure 6), the inertia value of the CAD® model is adequately exact and is $I_{rw} = 0.028 \quad (\text{kg m}^2)$.

The SADS needs to be manually balanced before any automatic balancing. By adequately exciting, the mass properties of the SADS could be deduced from attitude data and, hence, the platform should rotate around all three axes simultaneously such that sinusoidal maneuver is produced by three reaction wheels and an accurate controller. A quaternion-based PD control is developed for attitude maneuver where the proportional gain (Kp) and derivative gain (Kd) are set to 0.5 and 0.88, respectively. In order to investigate the results of identification properties by two methods (CLM and RLS) in a different situation, various maneuvers (five tests) with diverse amplitude and frequency have been applied to the SADS. Figure 7 shows the time history of experimental Euler angles for a sample maneuver. This maneuver is used as excitation for identification. Also, the angular velocities of reaction wheels during this maneuver are presented in Figure 8.

The distance between the CG and the CR and the moment of inertia by using the Euler angles and angular velocities of the SADS are measured.

The measurement accuracy of the AHRS is about 2° and 0.25°/s for angle and angular velocity, respectively. The step size in all simulations is 0.2 s. The error of the time synchronicity may result in inaccuracy of

the estimation. In order to start up a recursive algorithm, the initial values for inertia and mass center must be specified.

These values for inertia tensor and mass center are [3, 12, 12, 0, 0, 0] and [0, 0, 0], respectively, for whole experiments.

The results of the identified parameters using the RLS approach during five maneuvers are reported in Table 2.

As can be seen in Table 2 the estimation of properties during these maneuvers is clearly different from one another. We have endeavored to find main reasons for this challenging issue and three significant factors have been obtained for this objective; firstly, sample time of the maneuver is large and influences on the estimation result. Also, there is aerodynamic disturbance torque that affects on the convergence of the results. Moreover, when the reaction wheels operate at high angular velocity, the side plates of the SADS start to vibrate and disturbance from the platform is another problem. Based on these results we could not decide about values of mass properties. This problem has been reported in the satellite simulator for Virginia Tech and INPE Institute.[10,17]

The results of the identified parameters using the CLM approach during these five maneuvers are reported in Table 3.

These results are near to each other and are a proper reason to ensure the validity in data. The identified parameters have sufficient convergence during 5 tests, since the CLM method is a offline technique and estimates the properties based on the volume of data during the entire maneuver. These results indicate that CLM is less sensitive to disturbances and uncertainties.

As expected, because of the dumbbell shape of the SADS, the moment of inertia around the roll axis is less than the other axes. Also, the yaw and pitch inertia are approximately equivalent.

The manual balancing has proved to be effective since the CM is of the order of a tenth of a millimeter. The negative value for r_z indicates that the CM is below the CR, which makes the platform acting like a pendulum.

The outputs of the SADS dynamics model are used to validate the estimated parameters. As described in Figure 9, the inputs of the SADS dynamics model are the average estimated parameters—obtained from CLM approach—and the true values of reaction wheels speed. The process of validation data from CLM method is presented in Figure 9.

The comparison of outputs (angular velocities) of the SADS during real maneuver and simulation by estimated data from CLM technique are presented in Figure 10.

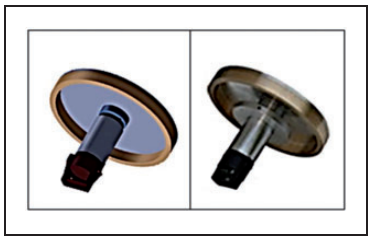

Figure 6. Real (right) and modeled (left) reaction wheel.

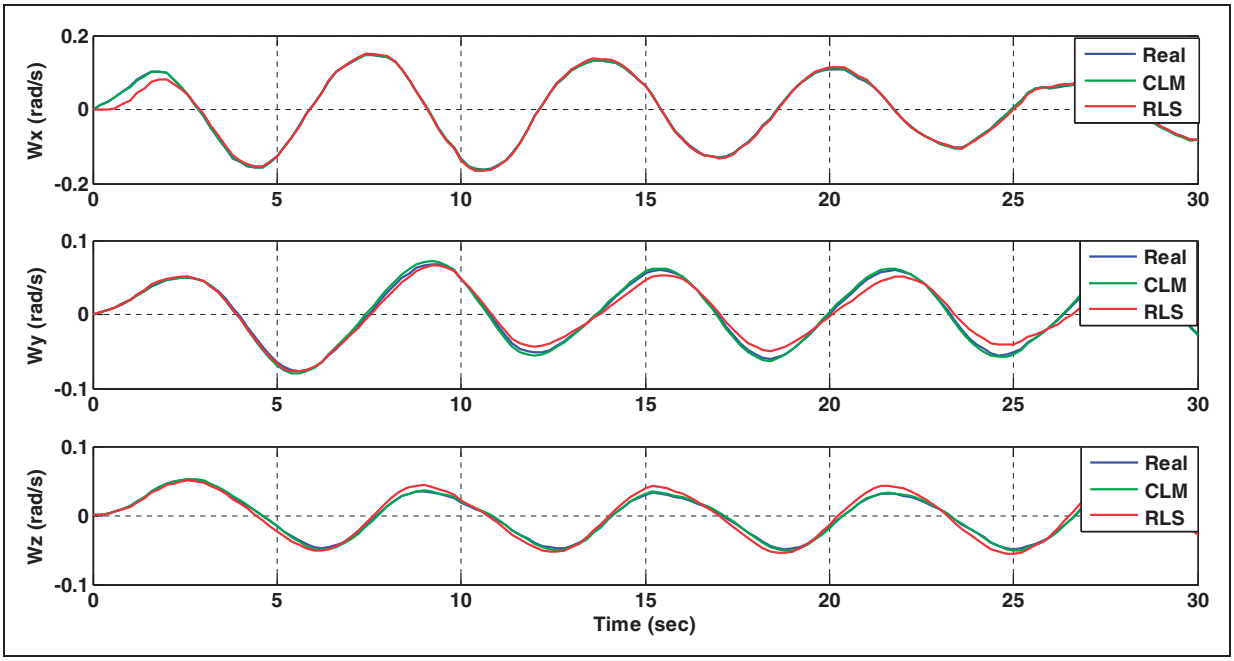

Figure 5. Comparison of CLM and RLS simulation results against desired data.
CLM: classical Levenberg–Marquardt; RLS: recursive least squares.

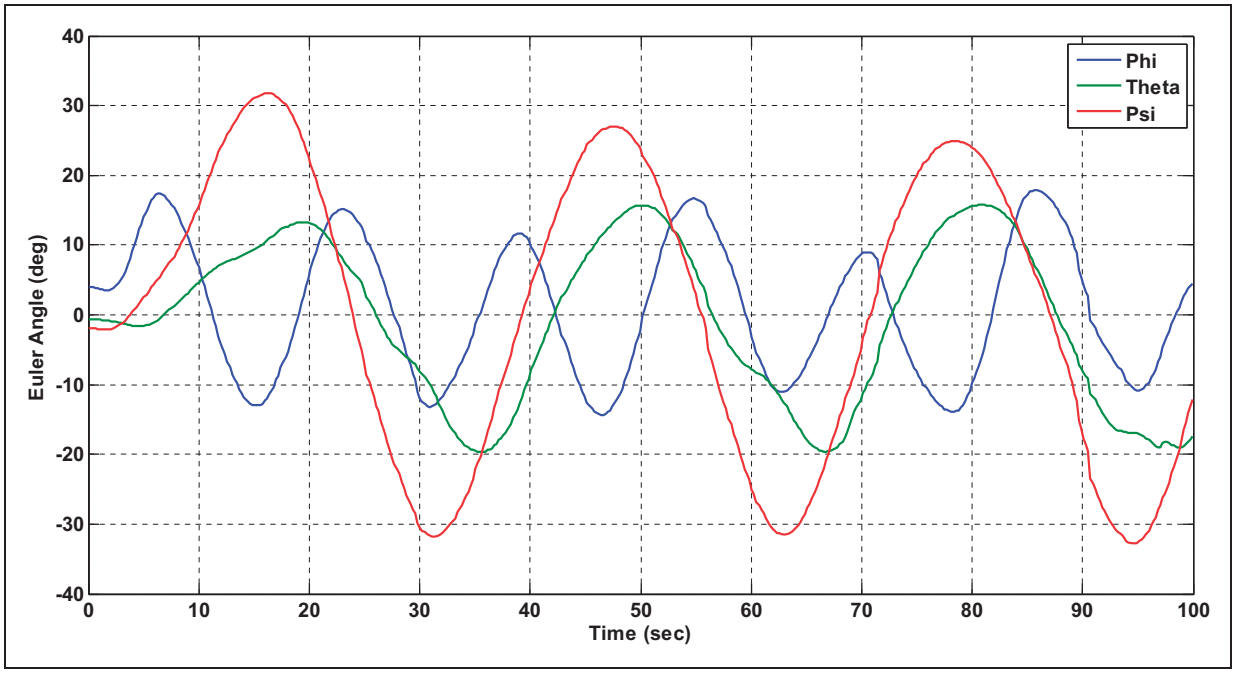

Figure 7. Experimental maneuver about three axes.

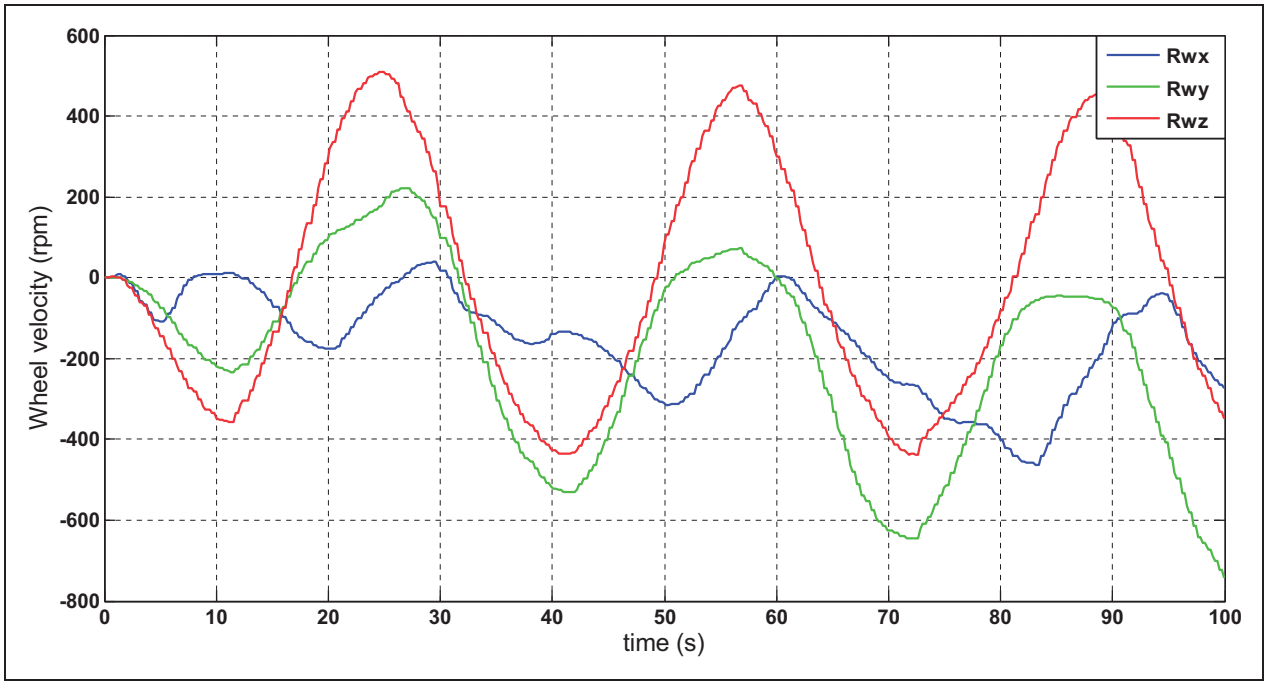

Figure 8. The angular velocities of reaction wheels during attitude maneuver.

Table 2. Experimental results for RLS methods.

Technique	Test	Ixx	Iyy	Izz	Ixy	Ixz	Iyz	Rx	Ry	Rz
RLS	1	2.8	11.8	12	1.6	−0.9	1.09	−9.7e-05	1.38e-04	−1.32e-04
	2	4	6.5	14.1	1.3	−0.81	1.32	−1.23e-04	2.5e-04	−0.94e-04
	3	1.2	10.1	13.9	2.5	−0.76	0.65	−1.1e-04	4e-05	−2.8e-04
	4	2.5	11.6	10.6	2.9	−1.5	1.87	−2.3e-04	1.86e-04	−1.7e-04
	5	3.5	14	16	0.8	−2.1	1.52	−3.1e-04	2.3e-04	−1.71e-04

RLS: recursive least squares.

Table 3. Experimental results for CLM methods.

Technique	Test	Ixx	Iyy	Izz	Ixy	Ixz	Iyz	Rx	Ry	Rz
CLM	1	2.95	12.34	12.38	1.36	−0.79	1.08	−1.19e-04	1.34e-04	−1.09e-04
	2	2.83	12.1	12.2	1.52	−0.85	1.12	−1.4e-04	1.5e-04	−0.94e-04
	3	3.1	12.02	12.25	1.54	−0.71	1.22	−1.24e-04	1.48e-04	−1.2e-04
	4	2.9	12.24	12.42	1.46	−0.69	1.19	−1.32e-04	1.38e-04	−1.11e-04
	5	2.87	12.19	12.19	1.41	−0.76	1.23	−1.35e-04	1.42e-04	−1.17e-04

CLM: classical Levenberg–Marquardt.

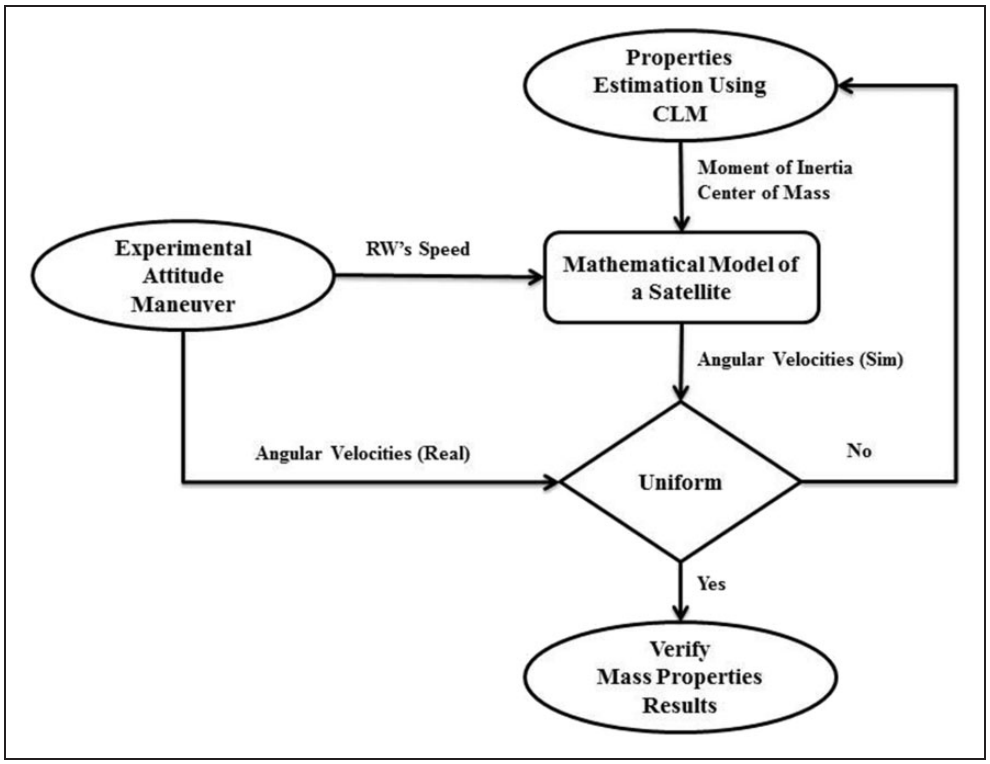

Figure 9. Validation process for CLM method.
CLM: classical Levenberg–Marquardt; RW: reaction wheel.

As illustrated in Figure 10, proper results are obtained with the CLM method because it produces a satisfactory fit in all directions and it proves that approach is low sensitive to the noises and uncertainties.

The estimated angular velocities do not exactly match the SADS real data, but this is because there are many uncertain disturbances that have not been considered in the simulation.

Mass balancing process

The gravitational torque as significant disturbance is produced by the existing offset between CM and CR that is calculated as

$$T_g = \vec{r} \times M\vec{g} \tag{17}$$

where M is total mass of the system with 95 kg and $\vec{r}$ is the position of the CM that has been calculated by using CLM approach with its results presented in Table 3; therefore the amount of external torque is calculated by equation (17).

The change in the position of the AMBS is defined as

$$Mr_i + md_i = 0 \quad (i = x, y, z) \tag{18}$$

where m is the balance mass and d is the distance that each balance mass requires to move.

By substituting the quantity of the offset $(\vec{r})$ and total mass M in equation (18), the distances that balance masses at each direction should move are determined.

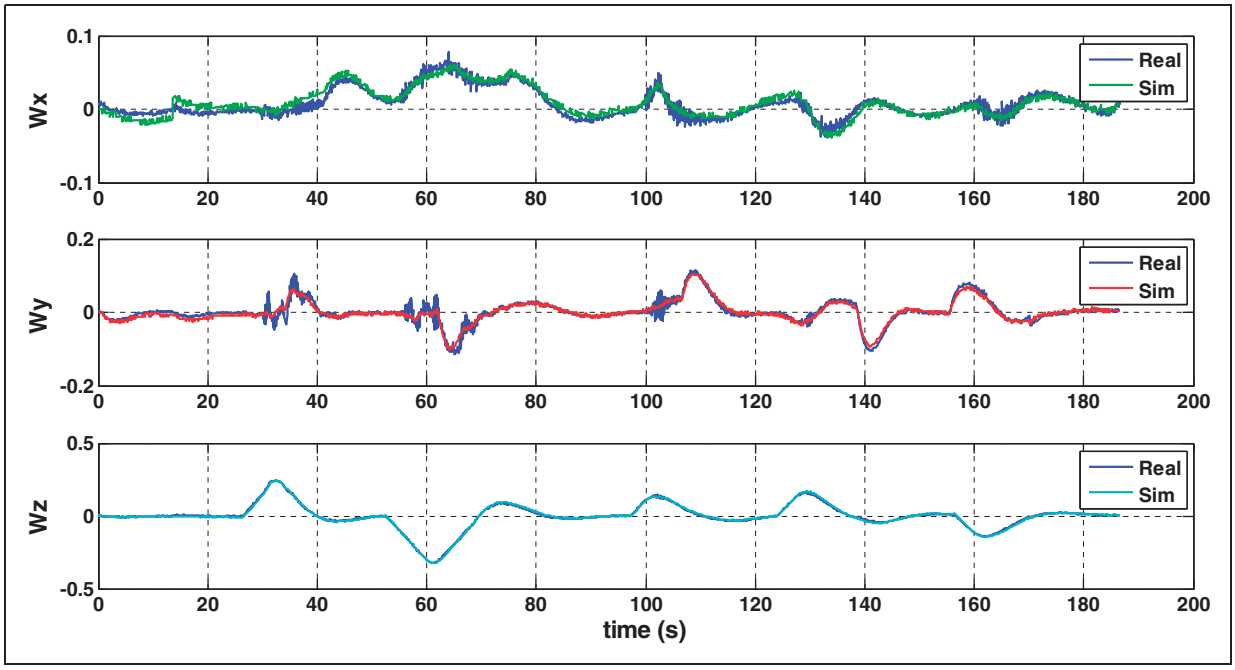

Figure 10. Real data of the SADS's angular velocities compared to CLM results.

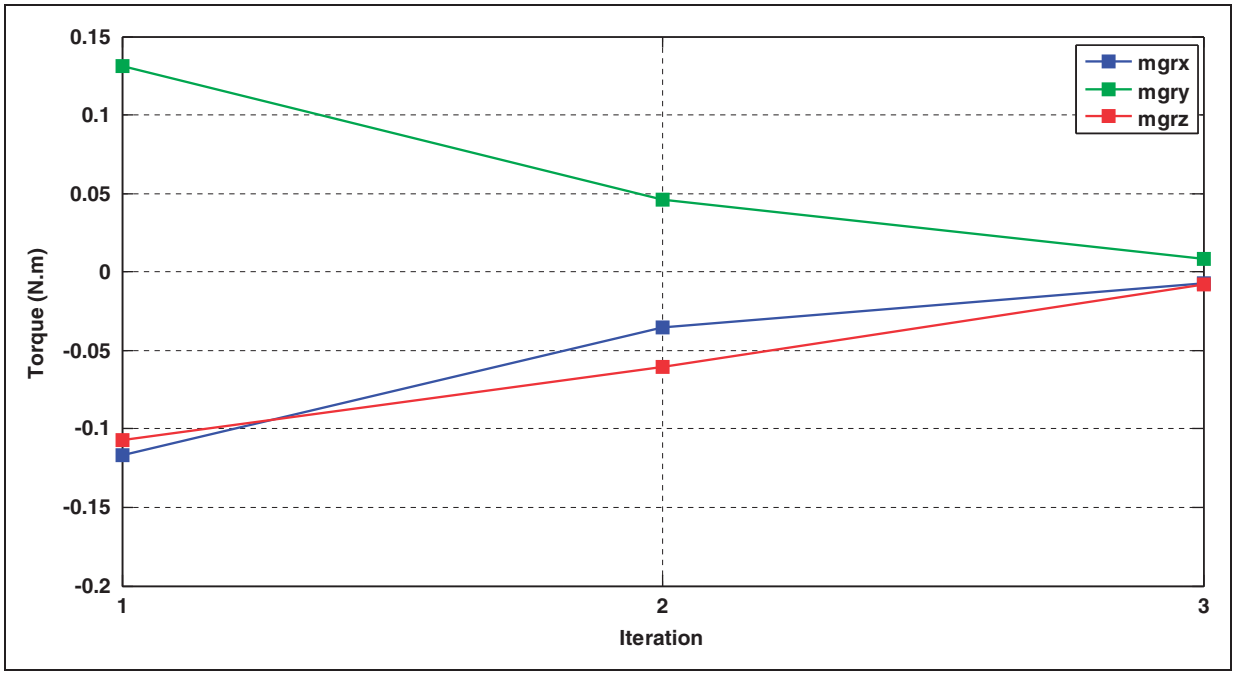

Figure 11. Iterative procedure of the AMBS.

The new location of balance mass is as follows

$$l = l_0 + d \tag{19}$$

where l_0 is the initial location and l is the final location of the balance mass.

The estimated results (Table 3) indicate that the CM and CR are very near to each other. In order to remove the offset between the CR and CM, the calculated changes are implemented via the AMBS.

For the purpose of decreasing the level of gravity torque, this procedure should be iterated. The changes of gravity torque for three iterations are shown in Figure 11 which illustrate how the gravity disturbance torque is decreasing through the balancing procedure.

AMBS moves the balance mass to the desired position to reduce the gap between the CM and CR, whereas the gravity torque falls to under 0.01 N m.

Conclusion

In this paper, estimation of mass properties was investigated through two techniques in order to develop the SRL SADS by the implementation and validation of the automatic balance system. For verification of the proposed methods, various experiments were performed with the SADS and the MATLAB®/SIMULINK® models. It has been demonstrated with the experiment results that the Classical Levenberg-Marquardt and Recursive Least Squares can be employed to identification mass properties of the SADS and results indicated that CLM technique is more convergence and reliable than RLS method. Furthermore, the results of estimation of the CM location were used by the AMBS to balance the platform which demonstrated enough performance. The advantage of the hardware-in-the-loop process for testing and validation provided a realistic demonstration of the expected performance of real systems.

Acknowledgements

The authors would like to thank the K. N. Toosi University of Technology, SRL for providing the space simulation environment.

Declaration of Conflicting Interests

The author(s) declared no potential conflicts of interest with respect to the research, authorship, and/or publication of this article.

Funding

The author(s) received no financial support for the research, authorship, and/or publication of this article.

References

1. Post MA, Li J and Lee R. Nanosatellite air bearing tests of fault-tolerant sliding-mode attitude control with Unscented Kalman Filter. In: *AIAA guidance, navigation, and control conference*, 13 August 2012, p.5040.
2. Horri NM, Palmer PL and Roberts M. Energy optimal spacecraft attitude control subject to convergence rate constraints. *Control Eng Pract* 2011; 19: 1297–1314.
3. Inumoh LO, Forshaw JL and Horri NM. Tilted wheel satellite attitude control with air-bearing table experimental results. *Acta Astronaut* 2015; 117: 414–429.
4. Hailey J, Sortun C and Agrawal B. Experimental verification of attitude control techniques for slew maneuvers of flexible spacecraft. In: *AIAA guidance, navigation and control conference*, 10–12 August 1992, pp.653–667.
5. Polo ÓR, Esteban S, Cercos L, et al. End-to-end validation process for the INTA-Nanosat-1B attitude control system. *Acta Astronaut* 2014; 93: 94–105.
6. Ousaloo HS, Nodeh MT and Mehrabian R. Verification of spin magnetic attitude control system using air-bearing-based attitude control simulator. *Acta Astronaut* 2016; 126: 546–553.
7. Kim JJ and Agrawal BN. Automatic mass balancing of air-bearing-based three-axis rotational spacecraft simulator. *J Guidance Control Dyn* 2009; 32: 1005–1017.
8. Smith GA. Dynamic simulators for test of space vehicle attitude control system. In: *Proceedings of the conference on the role of simulation in space technology, part C*, Virginia Polytechnic Institute and State University, Blacksburg, VA, 20–22 August 1964, pp.15-1–15-30.
9. Kim B, Velenis E, Kriengsiri P, et al. A spacecraft simulator for research and education. In: *Proceedings of the AIAA/AAS astrodynamics specialists conference*, Reston, VA, 30 July–2 August 2001, pp.897–914.
10. Schwartz JL and Hall CD. System identification of a spherical air-bearing spacecraft simulator. In: *Proceedings of the 14th annual AAS/AIAA spaceflight mechanics meeting*, 8–12 February 2004, AAS 04-122.
11. Small D and Zajac F. A linearized analysis and design of an automatic balancing system for the three axis air bearing table. In: *NASA TM-X-50177*, Goddard Space Flight Center, April 1963.
12. Ma O, Dang H and Pham K. On-orbit identification of inertia properties of spacecraft using a robotic arm. *J Guidance Control Dyn* 2008; 31: 1761–1771.
13. Bergman E and Dzielski J. Spacecraft mass property identification with torque-generating control. *J Guid Control Dyn* 1993; 13: 99–103.
14. Tanygin S and Williams T. Mass property estimation using coasting maneuvers. *J Guid Control Dyn* 1997; 20: 625–632.
15. Kim JJ and Agrawal B. System identification and automatic mass balancing of ground-based three-axis spacecraft simulator. In: *AIAA Guidance, Navigation, and Control Conference and Exhibit*, Keystone, Colorado, 21–24 August 2006.
16. Agnes GS and Fulton J. Design and Testing of SIMSAT, a three-axis satellite dynamics simulator. In: *Proceedings of the 19th AIAA Applied Aerodynamics Conference*, Anaheim, CA, USA, 11–14 June 2001, pp.01–1591.
17. De Oliveira AM, Kuga HK and Carrara V. Estimating the mass charcteristics of a dumbbell air bearing satellite simulator. In: Steffen Jr V, Rade DA and Bessa WM (eds) *Proceedings of the XVII International Symposium on Dynamic Problems of Mechanics*, Natal, RN, Brazil, 22–27 February 2015.
18. De Oliveira AM, Kuga HK and Carrara V. Estimating the mass charcteristics of a dumbbell air bearing satellite simulator. In: *22nd International Congress of Mechanical Engineering*, Ribeirao Preto, Brazil, 3–7 November 2013, pp.4836–4844.
19. Jung D and Tsiotras P. A 3-DoF experimental test-bed for integrated attitude dynamics and control research. In: *AIAA guidance, navigation, and control conference*, Austin, Texas, 11 August 2003.
20. Wenfu X, Yong H, Xueqian W, et al. On orbit identification of mass characteristic parameters for spacecraft. *J Astronaut* 2010; 31: 1906–1914.
21. Mirshams M, et al. Spacecraft attitude dynamics simulator actuated by cold gas propultion system. *Proc IMechE, Part G: J Aerospace Engineering* 2015; 229: 1510–1530.
22. Sidi MJ. *Spacecraft dynamics and control: A practical engineering approach*. Cambridge: Cambridge University Press, 1997.

23. Duncan DB and Horn SD. Linear dynamic recursive estimation from the viewpoint of regression analysis. *J Am Stat Assoc* 1972; 67: 815–821.
24. Haykin S. *Adaptive filter theory*. 3rd ed. Upper Saddle River, NJ: Prentice-Hall, Inc., 1996.
25. Levenberg K. A method for the solution of certain non-linear problems in least square. *Quart Appl Math* 1944; 2: 164–168.
26. Lourakis MIA. A brief description of the levenberg-marquardt algorithm implemented by Levmar. *Found Res Technol* 2005; 4: 1–6.
27. Marquardt DW. An algorithm for least-squares estimation of nonlinear parameters. *J Soc Ind Appl Math* 1963; 11: 431–441.